SHELL THICKNESS EVALUATION IN THE CONTINUOUS CASTING BY WEDGE METHOD *

Rafael Fernandes Reis[1]
Rodrigo Seara Martins[2]
Rodrigo Madrona Dias[3]
Vinicius Karlinski de Barcellos[4]

Abstract

The shell thickness is an important variable to achieve process control in continuous casting. The thinner solidified shell thickness at mold exit might induce a breakouts events or bulging. The knowledge of the solidification final point position allows to adjust cooling conditions intending less central segregation. In this paper, a methodology was developed and applied to evaluate solidified shell thickness by the wedge method. Cracks induced by the wedge, which are not visible to the naked eye, were revealed by immersion in a 13% ammonium persulfate reagent. The etch by immersion was preceded by milling and sanding procedures aiming to obtain a more homogeneous etched surface. The wedge technique allowed the measurement shell thickness up to 122 mm out of a total of 126 mm, which corresponds to 97% of the solidification process, showing robustness to evaluate the process in situ. It was noticed the precipitation of manganese sulfide aligned with the cracks and the formation of phases richer in carbon around of them. The correlation analysis of the main process parameters allowed to identify the effect of casting speed on the solidified shell thickness. A satisfactory coefficient of determination (R^2) equal to 0.71 was obtained for the industrial experiments carried out with different steel grades.

Keywords: Shell thickness; wedge method; continuous casting.

[1] *Metallurgical Engineer, M.Sc., Senior Researcher, Research and Development Center, Usinas Siderúrgicas de Minas Gerais-Usiminas, Ipatinga, MG, Brazil.*
[2] *Production Engineer, M.Sc., Production Engineer, Steelmaking Department, Usinas Siderúrgicas de Minas Gerais-Usiminas, Ipatinga, MG, Brazil*
[3] *Metallurgical Engineer, M.Sc., Production Specialist, Steelmaking Department, Usinas Siderúrgicas de Minas Gerais-Usiminas, Ipatinga, MG, Brazil*
[4] *Metallurgical Engineer, D.Sc., Professor, Metallurgical Department, Federal University of Rio Grande do Sul, Porto Alegre, RS, Brazil.*

** Technical contribution to the 52º Seminário de Aciaria, Fundição e Metalurgia de Não-Ferrosos, part of the ABM Week 7th edition, August 1st-3rd, 2023, São Paulo, SP, Brazil.*

1 INTRODUCTION

The continuous casting process is known for productivity and excellent cast products quality. These characteristics are associated with the high ability of controlled heat-removal process. In general terms, thermal homogeneity is sought along the casting strand and final point of solidification constancy position, to avoid the occurrence of internal and superficial defects and segregation. Furthermore, loss of heat removal might generate a thin shell thickness, unable to withstand ferrostatic pressure, leading to events that can cause breakout.

There are several techniques for measuring solidified shell thickness directly, such as: nail shooting, tracer dispersion, breakout event and wedge test. Nail shooting technique consists of the insertion by pressurized air of a nail in the strand in solidification, in the remaining liquid steel, a FeS_2 tracer is added to facilitate visualization after preparation [1-6]. Nail shooting has high acceptance due to the high frequency of successful tests, however it requires a considerable infrastructure to be assembled. An advantage of nail shooting is the possibility of measuring in more than one location along the width [7]. Li *et al.* [8] added FeS_2 to the mold surface and evaluated the dispersion to determine the solidified thickness. Thus, it can be validated from meniscus of the mold output vicinity, depending on the tracer added amount. Wang *et al.* [1] validated a numerical model by thickness measuring using the nail shooting technique and proposed a cooling plan with corner temperatures in the bending and unbending region outside the critical temperatures for cracking. Electromagnetic stirrer (F-EMS) employed in a certain position of the CC strand modifies the microstructure formed, being used as an indirect technique for solidified thickness measurements [9,10]. Petrus *et al.* [11] developed an indirect technique for solidified thickness determination by means of casting speed control rollers. The technique consists of moving outer rollers from the strand, monitoring the rotation when they approach the rollers again, then casting speed varied intending the shell approaching and withdrawing from the roller, then knowing the solid end point. One of the first techniques to be applied were those obtained under breakout conditions, where solidified thickness remaining is used after liquid steel leakage [12-16].

The thickness measurement can also be performed using the wedge technique, where a wedge is inserted between the strand and the roll, inducing cracks in the solidification front [17-19]. After cutting, sanding and etching by immersion in ammonium persulfate solution, cracks are revealed and the depth is considered as the thickness at the meniscus distance of wedge insertion.

Sengupta *et al.* [17] applied wedge test evaluating casting speed by shell thickness measurements. Wedge dimensions were: 25 mm for width and 6 mm for thickness.

The wedges were inserted at straightening end. The authors assumed for the calculations that shell thickness represents 0.7 of solid fraction at the mushy zone. Samples were machined, sanded and cracks revealed by an immersion sequence in ammonium cupric chloride solution. It has concluded that shell thickness decreases with casting speed increase for modeling and experimental results. In addition, the results compared individually at the same casting speed indicate that the model used to calculate the solidified thickness is close to the measured one, with a divergence of around 7%.

Michelic *et al.* [18] developed, implemented and validated a transient solidification and cooling model for blooms at Donawitz, in Austria. The solidified shell thickness validation part was evaluated by the wedge method. The authors do not inform the

distance from the meniscus where the measurements were taken, they only mention that it was treated by secondary cooling. They also conclude that shell thickness decreases with casting speed increase and almost linear profile. Shell thicknesses between 42 mm and 48 mm were measured at casting speeds ranging from 0.5 m/min to 0.65 m/min.
Louhenkilpi, Miettinen and Holappa [19] used the wedge technique to validate the TEMPSIMU® model in a slab casting machine. The researchers inserted 4 wedges in the same heat along the strand, at distances between 13 m and 20 m from the meniscus, at a speed of 1.30 m/min to determine the solidified thickness.
Therefore, in this article, we aimed to determine shell thickness by the wedge method in Usiminas machines. Furthermore, to evaluate the effect of casting speed and the main variables on the solidified shell thickness.

2 DEVELOPMENT

2.1 Materials and Methods

In the Figure 1 the wedge used with its main dimensions is shown in an isometric view.

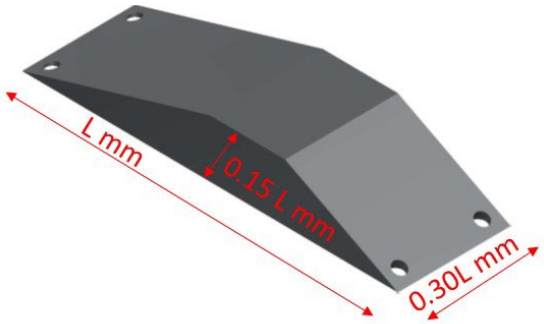

Figure 1. Three-dimensional wedge view.

The steel chemical composition selected to make the wedges is shown in the table 1. The wedges were heated until 900°C for 1 hour and cooled in water to obtain greater hardness.

Table 1. Wedge steel chemical composition (%)

Element	C	Mn	Si	Ni	Ti	Cr	Mo	Al	B	Nb
(%)	0.3	1.5	0.2	0.02	0.02	0.5	0.04	0.03	0.003	0.04

The distance from the meniscus for wedges insertion was 17 m, at the straightening end between segments 6 and 7 as showed in Figure 2. The best positioning on the slab surface is obtained with the use of a string water moistened. Reaching strand surface, the longitudinal wedge alignment to the casting direction is obtained by finally releasing the pair of strings closest to the mold, this detail favors the increase of the area penetrated by the wedge, avoiding side adhesion. The tests were done aiming less steel loss, so by phone contact, the cut operator indicated the moment to release de wedge and get the border slabs.

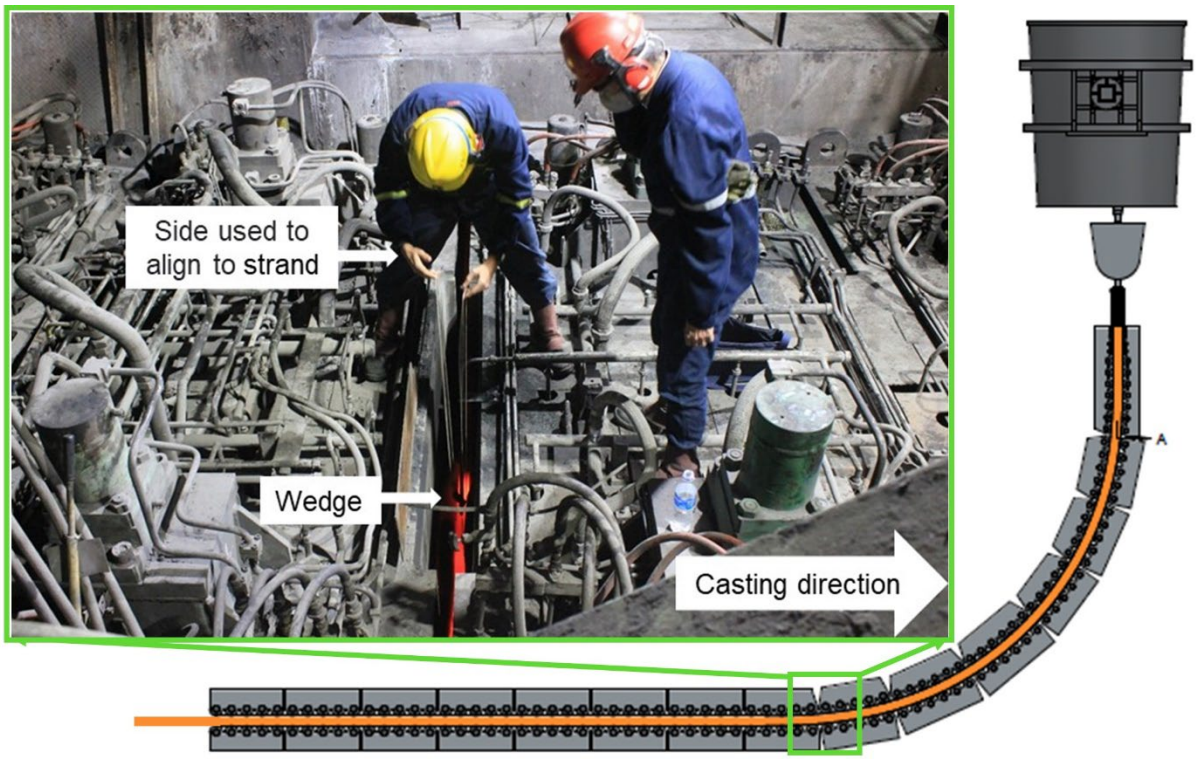

Figure 2. Photograph and details of the wedge insertion at the continuous casting machine.

Figure 3 shows a schematic drawing of wedge method between the first roll pair in two moments. Figure 3 a) shows the wedge being positioned over strand, showing the liquid and solid portions. After wedge release, in Figure 3 b), the roll presses the wedge on the strand, causing internal cracks at the solidification front. The distance from the slab surface until revealed crack tip is interpreted as shell thickness (s).

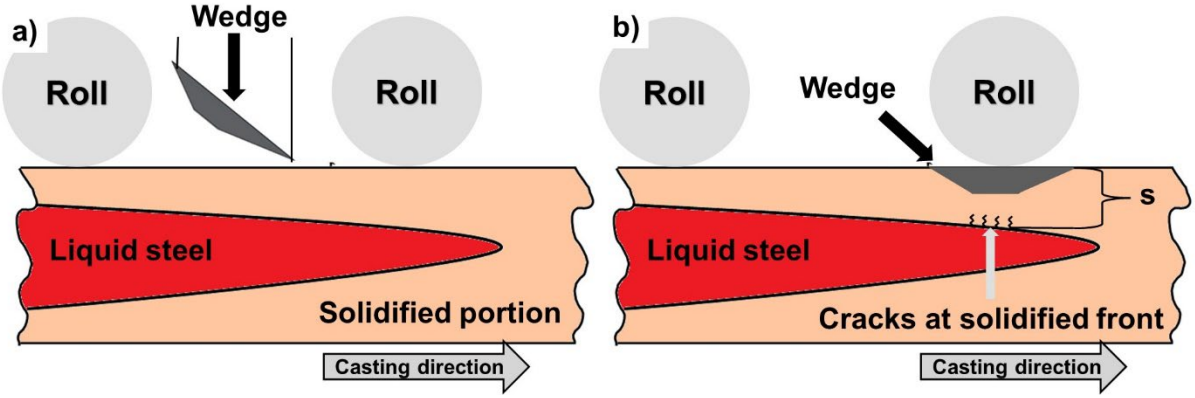

Figure 3. Schematic design of the wedge test: a) before adhesion and b) after adhesion.

Wedge adhered to the end of continuous casting machine is showed at Figure 4 a). And-after slab cut, in Figure 4 b), it is showed near the border sample position.

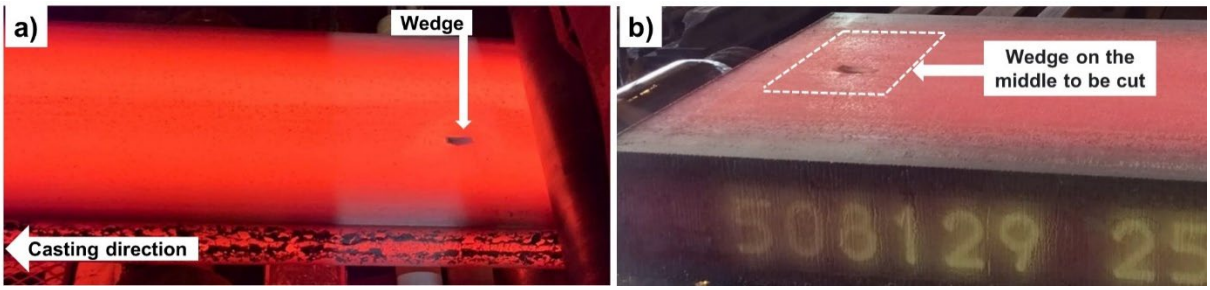

Figure 4. Wedge view at a) end of casting machine and b) after slab cutting.

The Figure 5 a) shows an example of the block sampled on the slab, after wedge inserted, highlighting the cut dotted lines in red. At this stage, it is important to remove the wedge from the sample due to the high hardness of the piece, which could damage the saw teeth and, in addition, allow the wedge to be reused for other tests. Figure 5 b) shows next cutting sequence, three parts were removed as evidenced by dotted red lines, decreasing machining area.

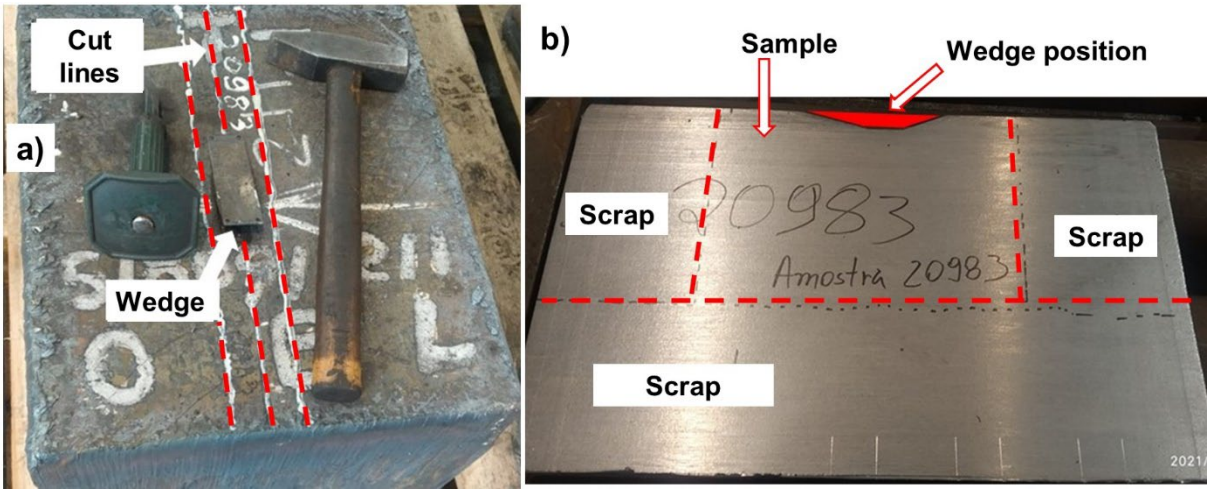

Figure 5. Wedge photograph of the region after sampling (a) in the slab and (b) of the section after cutting.

After cutting process samples were subject to milling cutters methods aiming a better finishing surface. And then, samples were immersed in a solution of oil remove. The macro etchings were done by immersion in until cracks revelations.

2.2 Results and Discussion

Figure 6 shows experimental results obtained by macro etching for heat number 538926. Each side of wedge adhesion were evaluated and receiving letter A and B. The distance between cracks and surface were treated as shell thickness (S). The mean and standard deviation for the sample 538926 was 114 mm ± 7 mm. Heat 538926 was the first of the eight and slab 241 with the wedge test is the 4th plate on the strand, so it could not represent steady state. The mushy zone was measure by the distance between red and green horizontal lines, obtaining 6.8 mm and 7.1 mm for A and B, respectively.

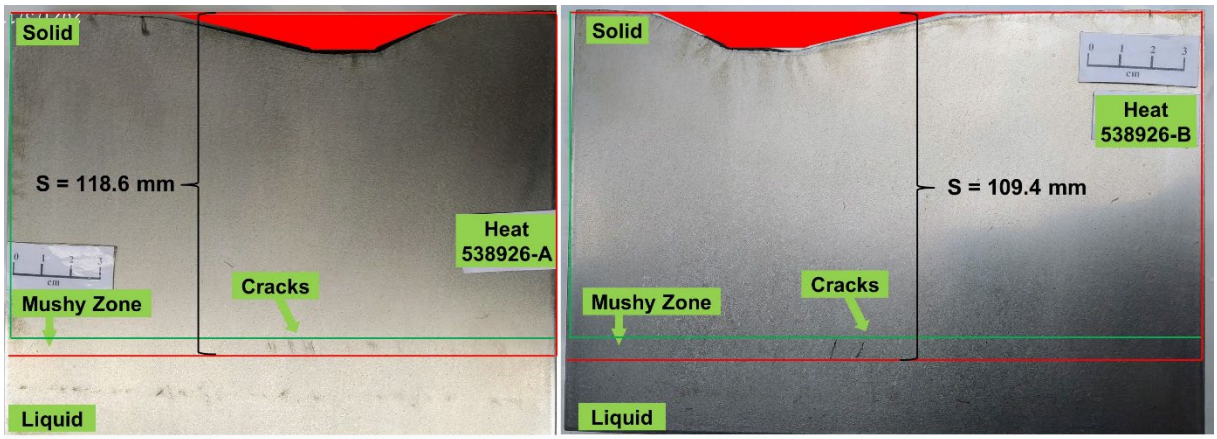

Figure 6. Macro etching results obtained for medium carbon steel deoxidized to aluminum and silicon – heat № 538926.

Cracks region on number 538926-B were analyzed by optical microscopy to measure and confirm positions. Figure 7 a) shows regions as polished and 7 b) etched by nital 4%. The polished results confirmed the cracks presence that were not visible without exposure via macro etching. The crack length is showed equals to 5.98 mm in Figure 7 b). The cracks extensions compared by macro etching and optical microscopy demonstrates good approximations, considering errors between these techniques. Ferrite and perlite were identified by nital and in the vicinity of cracks higher fraction of carbon-rich constituents once darker coloration is observed.

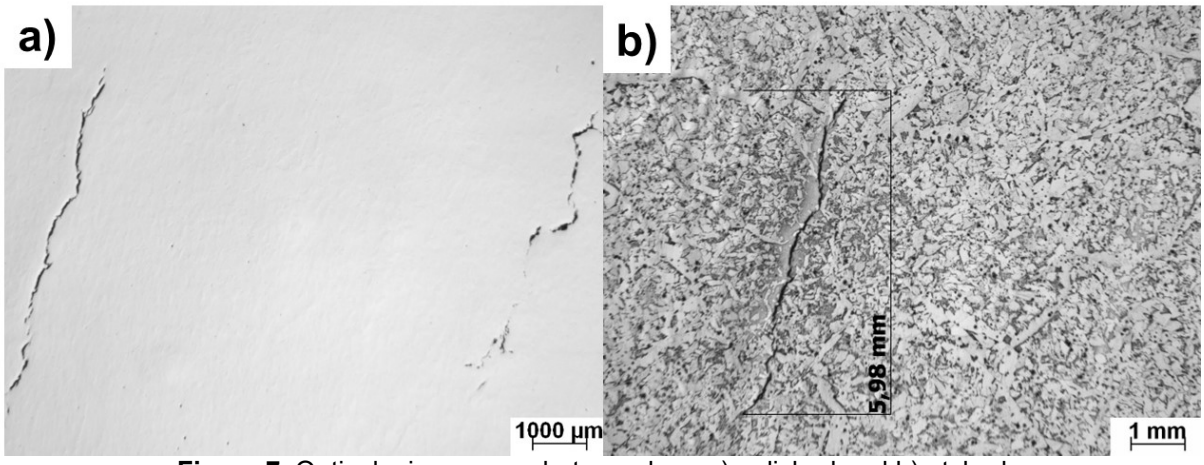

Figure 7. Optical microscopy photograph as a) polished and b) etched.

Figure 8 presents cracks for heat № 436777. The mean and standard deviation obtained were 122 mm ± 1 mm, respectively.

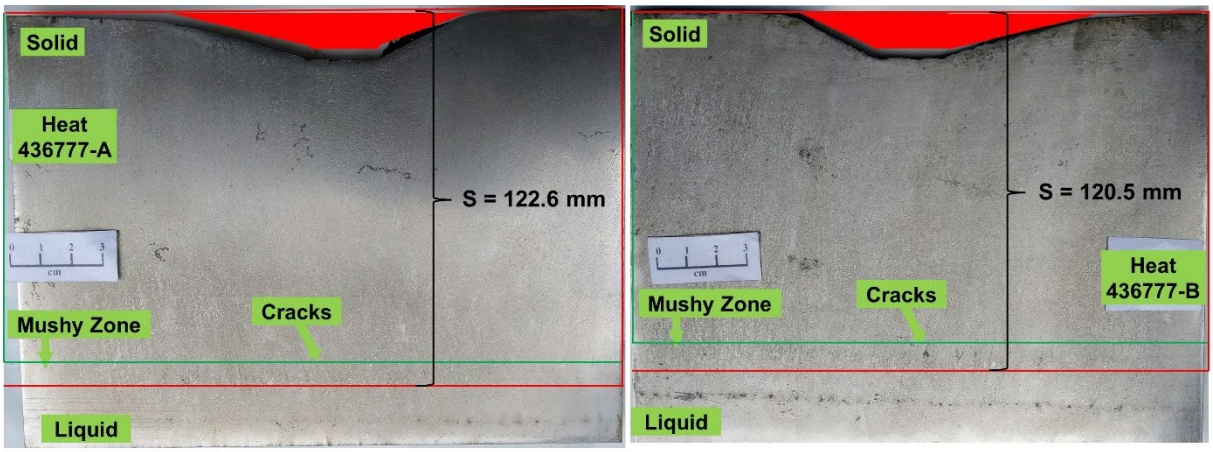

Figure 8. Macro etching results obtained for medium carbon steel deoxidized to aluminum – heat № 436777.

Figure 9 shows the results for heat № 442629, average thickness found, and the standard deviation were 113 mm ± 1mm for the sample that corresponds to a low carbon steel.

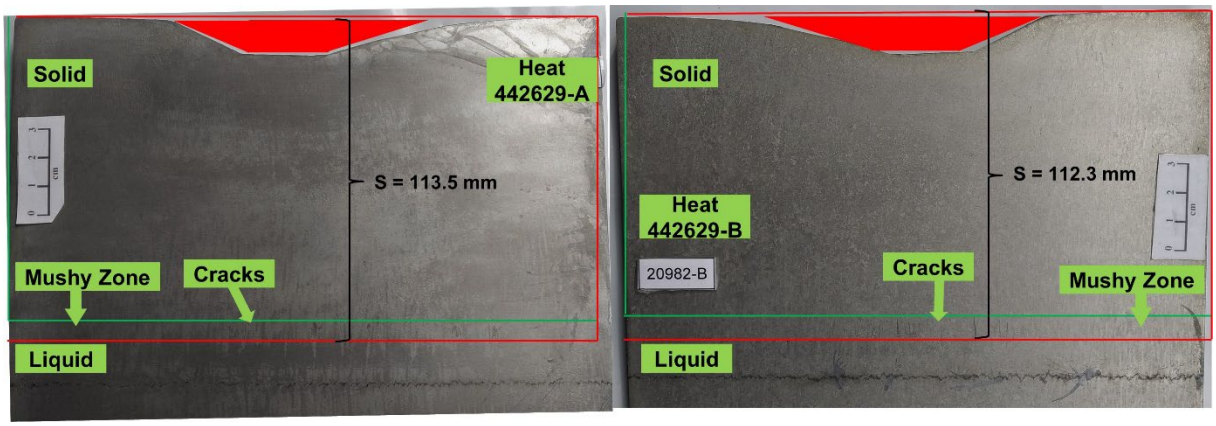

Figure 9. Macro etching results obtained for low carbon steel deoxidized to aluminum – heat № 442629.

The cracks on sample of face b and heat № 442629 were investigated using a scanning electron microscope. An energy dispersive spectroscopy (EDS) map was done, and results are show at Figure 10. It was identified substantial concentration of elements Mn and S in the crack, suggesting MnS formation.

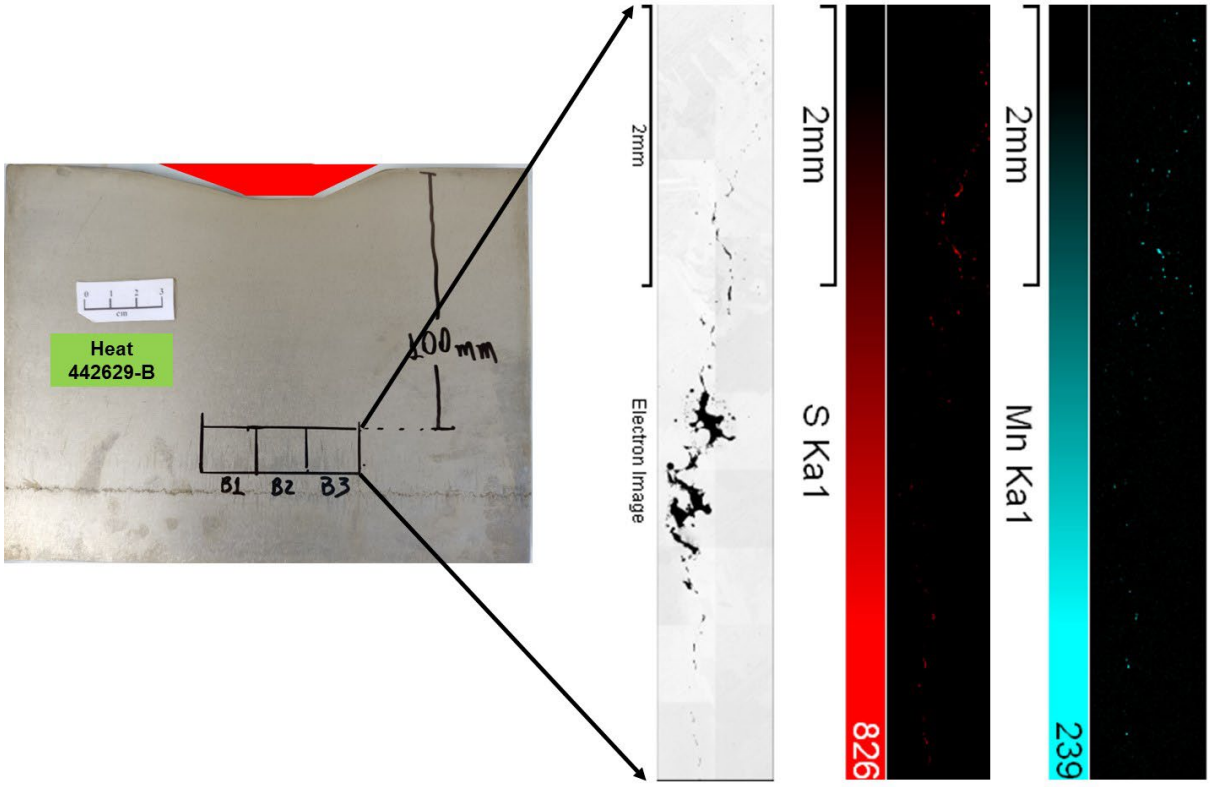

Figure 10. Microscopy electrical results obtained for cracks regions.

Figure 11 shows shell thickness results in a low carbon steel at heat № 546325. The average and standard deviation is 121 mm ± 1 mm.

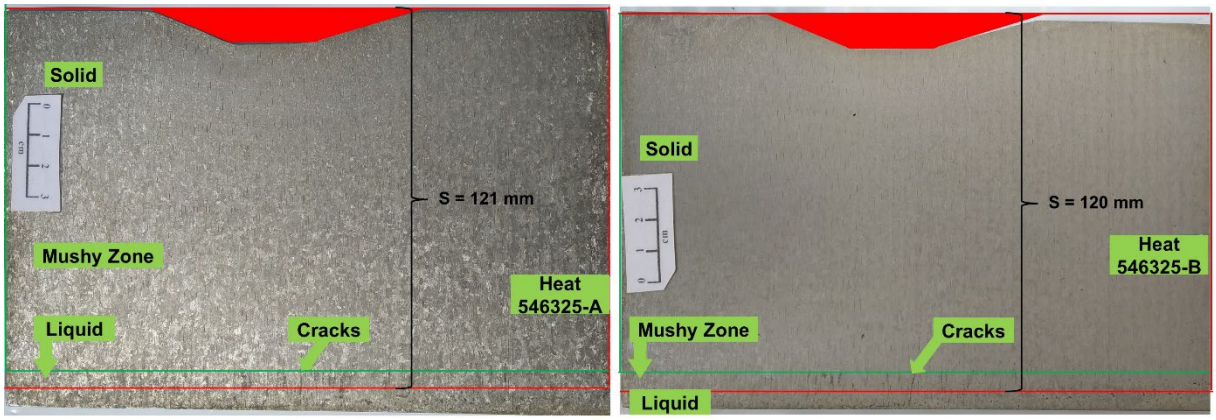

Figure 11. Macro etching results obtained for low carbon steel deoxidized to aluminum – heat № 546325

Figure 12 shows shell thickness results in a high carbon steel at heat № 551052. The average and standard deviation is 109 mm ± 1 mm.

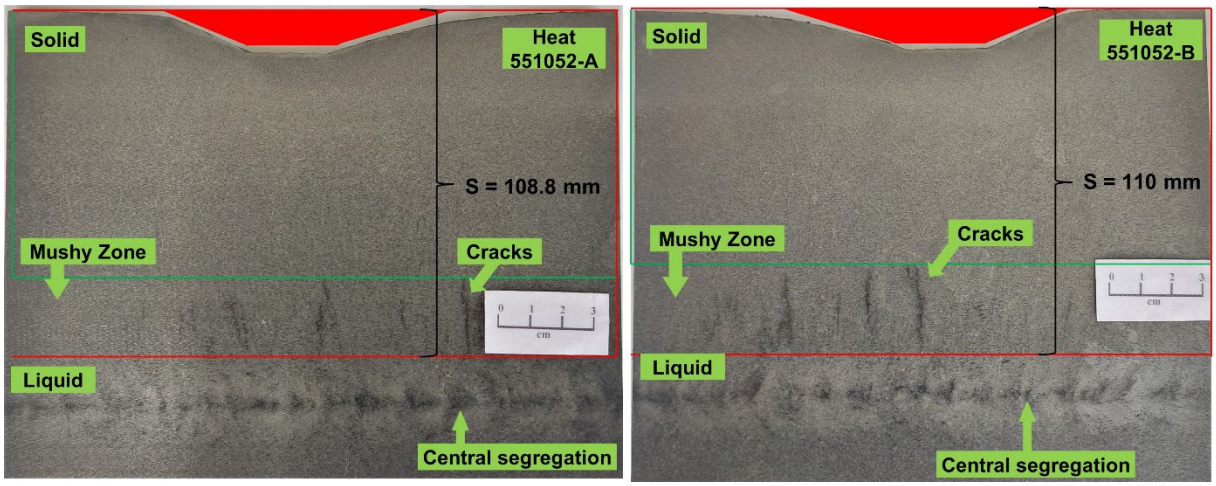

Figure 12. Macro etching results obtained for high carbon steel deoxidized to silicon and aluminum – heat № 551052

Figure 13 shows macro etching results for heat № 257607. It was not evidenced cracks, meaning that it was completely solidified at 17 m from meniscus.

Figure 13. Macro etching results obtained for low carbon steel deoxidized to aluminum – heat № 257607

It is known that under normal cooling conditions between the wide faces, the final point of solidification occurs at half slab thickness, so for Usiminas, currently with 252 mm slabs, there is 126 mm. This study has shown cracks of up to 121 and 122 mm in depth, proving the robustness of wedge method for evaluating solidified shell thickness.

The table 2 was constructed intending to evaluate process parameters influencing on shell thickness and *s* is shell thickness, *cs* is casting speed, *W* is slab width, *CE* is carbon equivalent, *SH* is super heat (degrees above *liquidus* temperature) and *WF* is water flow.

Table 2. Average shell thickness and process parameters analyzed

	Variables					
Heat number	**s [mm]**	**cs [m/min]**	**W [mm]**	**CE**	**SH [°C]**	**WF [l/min]**
538926	114	0.78	905	38	19	1253
436777	122	0.70	1223	41	33	1308
442629	113	0.90	1445	10	30	1682
546325	121	0.80	1325	8	32	3263
551052	109	0.89	1325	58	5	2020
257607	126	0.72	1565	9	27	2974

Carbon equivalent was calculated using Equation 1.

$$CE=C+Mn/6+Si/24+(Cr+Mo+V+Nb+Ti)/5+(Ni+Cu)/15+5B \quad (1)$$

A correlation analysis was conducted in commercial Minitab® statistics software between solidified shell thickness and process variables, with the results shown in Figure 14. Each graph has two parameters, p-value (p) that means hypothesis test result and r that represent strong linear correlation's Pearson. When p is less than 0.05 is statistically possible to affirm the linear correlation. It is noticed that was achieved only for casting speed a p less than 0.05, and the highest modulus correlation equals to -0.0842.

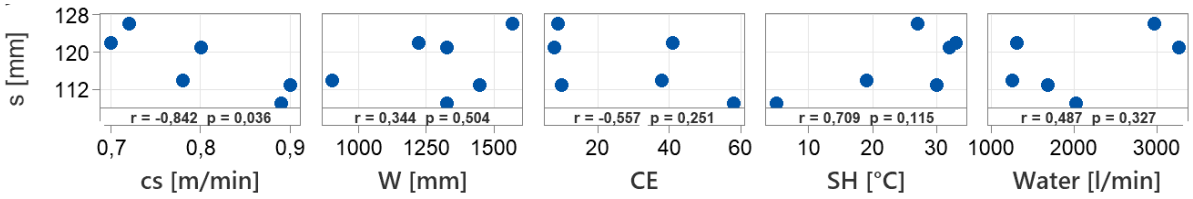

Figure 14. Correlation analysis results of shell thickness and process parameters.

The Figure 15 shows a graph comparing measured data and literature results of shell thickness as function of casting speed. Sengupta et al. [17] evaluated slabs in high casting speed conditions and, in another way, Michelic et al. [18] studied blooms in low speed. Although there are differences, especially for Sengupta et al. [17], the linear correlation and inverse effect is very close. Since the number of experiments was reduced, it may be that the influence of the other parameters would require a larger sample, in order to seek a good correlation between the data.

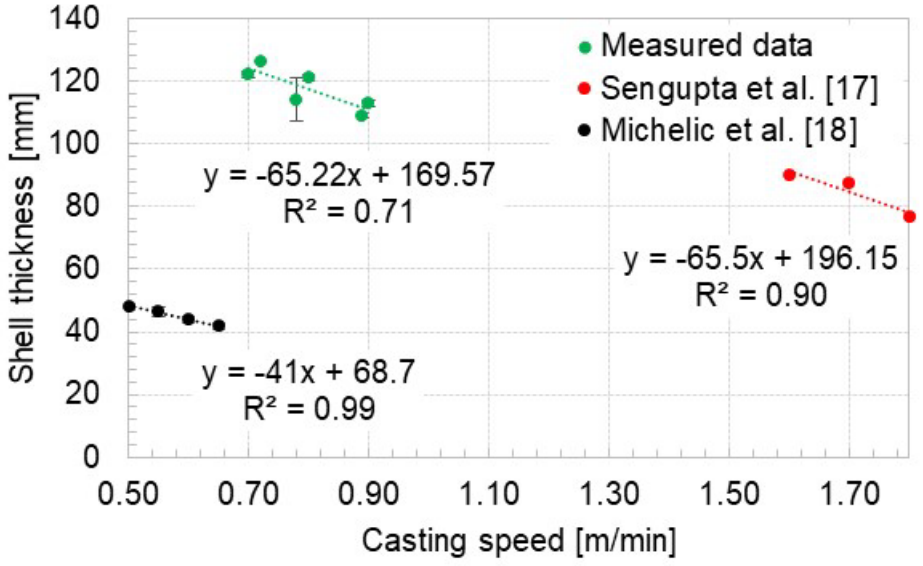

Figure 15. Shell thickness comparison between measured data and literature as function of casting speed.

3 CONCLUSION

A methodology was developed and applied to measure solidified shell thickness by the wedge method.

The wedge method allowed measurement of the shell thickness up to 122 mm for a total of 126 mm, that is, 97% of the solidification process, showing the robustness of the method.
Cracks not visible to the naked eye were revealed by immersion in 13% ammonium persulfate reagent. It was noticed the precipitation of manganese sulfide aligned with the cracks and formation of phases richer in carbon near cracks.
The correlation analysis of the main process parameters allowed identifying the effect of the casting speed on the solidified shell thickness. A satisfactory coefficient of determination (R^2 equal to 0.71) was obtained for the 6 industrial experiments, for the different steel grades.

REFERENCES

1 Y. Wang, Q. Ren, L. Zhang, X. Yang, W. Yang, Y. Ren, and H. Zhang, Steel Res. Int., 92, 2000649 (2021).
2 Y. Ito, T. Murai, Y. Miki, M. Mitsuzono, and T. Goto, ISIJ Int., 51, 1454–1460 (2011).
3 Yim, “Steelmaking conference proceedings. 81: Toronto Meeting, March 22-25, 1998”, Iron & Steel Society, Warrendale, Pa (1998).
4 J.C. Ma, H.Z. Sun, X.B. Wang, and X. Lv, Appl. Mech. Mater., 80–81, 81–85 (2011).
5 Y. Kong, D. Chen, Q. Liu, H. Chen, and M. Long, Steel Res. Int., 89, 1800091 (2018).
6 X.-Y. Liu, Z. Xie, J. Yang, H.-J. Meng, and Z.-Y. Wu, J. A faster than real-time heat transfer model for continuous steel casting, Journal of Materials Research and Technology, Volume 19, 2022, Pages 4220-4232.
7 M. Long, H.Chen, D. Chen, S. Yu, B. Liang, H. Duan. A Combined Hybrid 3-D/2-D Model for Flow and Solidification Prediction during Slab Continuous Casting. Metals. 2018; 8(3):182. https://doi.org/10.3390/met8030182D. Li, H. Wu, H. Wang, and H. Li, J. Iron Steel Res. Int., 27, 782–787 (2020).
8 L. Huicheng, Asp. Min. Miner. Sci., 6, (2021).
9 X. Chen, W. Deng, and S. Niu, Processes, 9, 2280 (2021).
10 B. Petrus, D. Hammon, M. Miller, B. Williams, A. Zewe, Z. Chen, J. Bentsman, and B.G. Thomas, Iron Steel Technol, 12, 58–66 (2015).
11 M. Alizadeh, S.A.J. Jahromi, and S.B. Nasihatkon, ISIJ Int., 50, 411–417 (2010).
12 J. Iwasaki and B.G. Thomas, Thermal-Mechanical Model Calibration with Breakout Shell Measurements in Continuous Steel Slab Casting, in: Ed. by Tms, Suppl. Proc., John Wiley & Sons, Inc., Hoboken, NJ, USA (2012), pp. 355–362.
13 K. Miłkowska-Piszczek, M. Rywotycki, J. Falkus, and G. Kwinta, Ironmaking and Steelmaking, 48, 1102–1109 (2021).
14 B. Santillana, B.G. Thomas, G. Botman, and E. Dekker, 9 (n.d.).
15 J. Zhang, D.-F. Chen, C.-Q. Zhang, S.-G. Wang, and W.-S. Hwang, J. Mater. Process. Technol., 229, 651–658 (2016).
16 J. Sengupta, M. Trinh, D.L. Currey, and B.G. Thomas, Utilization of CON1D at ArcelorMittal Dofasco’s No. 2 Continuous Caster for Crater End Determination, in: (2009).
17 S. Michelic, C. Bernhard, W. Rauter, M. Erker, W. Brandl, J. Reiter, and A. Sormann, 10 (n.d.).
18 S. Louhenkilpi, J. Miettinen, and L. Holappa, ISIJ Int., 46, 914–920 (2006).